Chemical Engineering Journal 166 (2011) 765–771

Contents lists available at ScienceDirect

Chemical Engineering Journal

journal homepage: www.elsevier.com/locate/cej

Defluoridation of water using calcined magnesia/pullulan composite

Jianxiong Kang, Bo Li, Jing Song, Daosheng Li, Jing Yang, Wei Zhan, Dongqi Liu*

School of Environmental Science and Engineering, Huazhong University of Science and Technology, No. 1037 Luoyue Road, Wuhan 430074, PR China

ARTICLE INFO

Article history:
Received 11 August 2010
Received in revised form 8 November 2010
Accepted 8 November 2010

Keywords:
MgO
Pullulan
Calcined MgO/pullulan composite
Defluoridation
Adsorption

ABSTRACT

In the present study, the performance of a novel adsorbent was investigated for fluoride removal from water. The adsorbent was synthesized by calcining magnesia (MgO) with pullulan, an extracellular water-soluble microbial polysaccharide, and characterized using FTIR, SEM, XRD and BET. The results showed that the surface area and the adsorption micropore of the calcined MgO/pullulan composite were increased from 7.5888 m^2/g and 13.91507 nm for pure MgO to 32.8992 m^2/g and 29.11552 nm, respectively. FTIR analysis showed that hydrogen bonds were formed in the adsorption of fluorides onto the calcined MgO/pullulan composite. At 30 °C and pH 7.0, the adsorption capacity was determined as 4537 mg/kg using an the initial concentration of 10 mmol/L fluoride solution. The adsorption capacity of calcined MgO/pullulan composite remained stable in the range pH 2–10. The adsorption isotherms fitted well to the Langmuir isotherm model. Thermodynamic parameters viz, ΔG°, ΔH° and ΔS° were measured as $\Delta G^\circ = -22.44\ kJ\ mol^{-1}$, $\Delta H^\circ = 0.58\ kJ\ mol^{-1}$, and $\Delta S^\circ = 0.093\ kJ\ mol^{-1}\ K^{-1}$, respectively. The adsorption kinetics of fluoride onto the calcined MgO/pullulan composite closely followed the Lagergren's pseudo-second-order rate mode, which indicates that the chemical adsorption, rather than mass transfer, is the rate-determining step.

1. Introduction

Fluoride is an essential micronutrient for humans but an excess intake (>1.0 mg/L) causes mottling of teeth, fluorosis (dental and/or skeletal) and several neurological disorders [1,2]. Therefore, drinking water with a fluoride concentration in excess of 1.5 mg/L requires defluoridation treatment [3].

Among the various methods based on the principles of precipitation [4], ion exchange [5], membrane diffusion [6], adsorption [7] and electrolysis [8] which have been proposed for removal of excess fluoride in drinking water, adsorption treatment was found to be the most efficient, due to the simple operation and the cheap absorbent. To date, a number of different adsorbents including activated alumina [9], activated carbon [10], lanthanum impregnated silica gel [11], calcite [12], clay [13,14], rare earths [15], and magnesia (MgO) [16] have been reported for the removal of fluoride in adsorption processes. In particular, MgO showed extraordinarily high defluoridation capacity. However, a minimum contact time of 1 h is required to reach maximum defluoridation capacity and the fine porosity necessitates also requires a greater back pressure to force the inert water through the small passages and interstices between the MgO particles [17].

Recently, a biocomposite adsorbent prepared from MgO and chitosan has been demonstrated to exhibit higher defluoridation capacity and reduced contact time relative to MgO [18]. Chitosan was found to contribute to the enhancement of defluoridation capacity by removing fluoride through hydrogen bonding between hydroxide radicals and fluoride ions (F^-) [17–20]. In this case, pullulan, a biocompatible, non-toxic and biodegradable extracellular water-soluble microbial polysaccharide produced by the fungus strain *Aureobasidium pullulans*, potentially has advantages as an adsorbant. The pullulan saccharide unit possesses more hydroxide radicals than the chitosan saccharide unit increasing the number of potential sites for adsorption. Furthermore, pullulan lacks the $-NH_2$ group of chitosan which may potentially serve as a nitrogen source for microorganisms in the treatment system. We here describe a novel composite prepared by the calcination of pullulan with MgO, and the effects of pH, dosage, initial fluoride concentrations, competitor anions and temperatures on fluoride removal efficiency are explored. Additionally, the nature and morphology of the calcined MgO/pullulan composite (cMgOP) was characterized by SEM with EDAX, XRD and FTIR. The adsorption process was also described using various kinetic models.

2. Materials and methods

2.1. Synthesis of cMgOP

Pullulan was purchased from TCI (Shanghai Branch, China). MgO and all other chemicals were of analytical reagent grade and used

* Corresponding author. Tel.: +86 27 87792512; fax: +86 27 87792172.
E-mail address: dongqiwh@yahoo.com (D. Liu).

1385-8947/$ – see front matter © 2010 Elsevier B.V. All rights reserved.
doi:10.1016/j.cej.2010.11.031

without further purification. To obtain a composite exhibiting both appropriate porosity for diffusion of the liquid and the better utilization of available actives for the adsorption of fluoride ions, MgO and pullulan were mixed by deionized water (ddH_2O) in the ratio of 4:1, 3:2, 1:1, 2:3 and 1:4 and then stirred for 24 h. The homogenous mixture was then dried at 80 °C in an drying oven and calcined at 450 °C in muffle furnace for 2 h to prepare cMgOP. Pure MgO and pullulan were subject to the same procedure as a control.

2.2. Adsorption studies

A stock solution of sodium fluoride (100 mg/L) was prepared with ddH_2O and further diluted to desired concentrations before use. The adsorption experiments were conducted by shaking the mixture in a thermostatic rotator at a speed of 200 rpm. The effect of different initial F^- concentrations at three different temperatures viz., 30 °C (303 K), 40 °C (313 K) and 50 °C (323 K) on extent of F^- removal was investigated by suspending 0.1 g cMgOP in F^- solutions with a volume of 50 ml at pH 7.0. At the end of adsorption period, the concentration of F^- in the residual solution was analyzed by the standard method of Fluorine reagents spectrophotometry. The pH at zero point charge (pH_{zpc}) of sorbents was measured using the pH drift method [21]. All water quality parameters were determined by using standard methods.

2.3. Instrumental studies

Scanning electron microscopy (SEM) and energy dispersive X-ray (EDX) analysis was performed using an FEI Quanta 200 scanning electron microscope. FTIR spectra of the samples were characterized using VERTEX 70/70v FT-IR spectrometers. X-ray powder diffraction (XRD) patterns were analyzed using a PANalytical B.V. X'Pert PRO X-ray diffractometer with Cu Kα radiation. The specific surface area of the composite was analyzed using the BET isotherm method with ASAP 2020 Accelerated Surface Area and Porosimetry System.

The data were processed using ORIGIN 6.0. The goodness of fit model was tested by using regression correlation coefficient (r) and χ^2-analysis.

3. Results and discussion

3.1. Characterization of the adsorbent

Adsorption of F^- to cMgOP was tested for composites composed of MgO and pullulan in the ratio of 4:1, 3:2, 1:1, 2:3 and 1:4 (MgO:pullulan). The composite in the ratio of 2:3 (MgO:pullulan) exhibited the highest defluoridation capacity and an appropriate diffusion of the liquid, cMgOP was henceforth synthesized by mixing MgO and pullulan in this ratio. The specific surface area of MgO and cMgOP was determined as 7.5888 m^2/g and 32.8992 m^2/g, respectively. The enlarged specific surface area increases the accessibility of the adsorbate-binding sites and thereby enhances the sorption of fluoride.

FTIR spectra were analyzed in order to determine the nature of the interaction between F^- and cMgOP. The FTIR spectra of cMgOP before (a) and after (b) treated with fluoride are shown (Fig. 1). According to the standard spectra, the band at 3701.25 cm^{-1} corresponds to –OH stretching vibrations of weakly H-bonded OH of water [22], and a significantly broadened stretching vibration band at 3441.66 cm^{-1} is assigned to the formation of the O–H···F bond [18] indicating the presence of hydrogen bonding. The bands at around 1475.40 cm^{-1} can be attributed to $-CH{=}CH_2$, with the stretching vibration disturbed by the presence of water molecules in the sample.

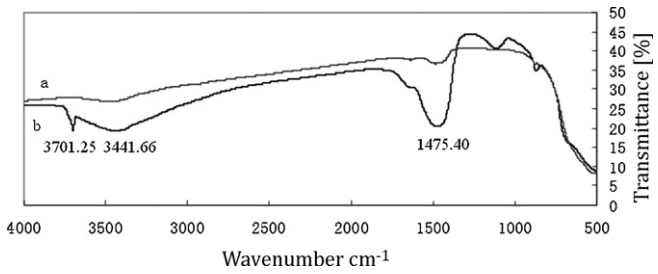

Fig. 1. FTIR spectra of (a) cMgOP and (b) fluoride-sorbed cMgOP.

SEM showed that the irregular-shaped particles of calcined pullulan (Fig. 2a) and MgO (Fig. 2b) were converted to a honeycomb-like surface structure (Fig. 2c) when cMgOP was formed. The honeycomb-like morphology of cMgOP was seen to be stable to fluoride adsorption, as no significant change can be found between the fluoride adsorbed and un-adsorbed samples (Fig. 2c and d). With this type of surface structure it is possible to maintain the high specific surface area of cMgOP and thereby endow it with a stable adsorption capacity. Furthermore, the enlarged porosity also decreases the back pressure required to force the inert water through the passages and interstices between the cMgOP particles. EDX spectra confirmed the presence of relevant elements in cMgOP before (Fig. 2e) and after treatment by the fluoride (Fig. 2f). It clearly indicated F element was introduced into cMgOP after adsorption.

The pH_{zpc} or zero point of charge is often used as an important parameter to analyze the electrostatic surface change [23]. In the present work, the pH_{zpc} of MgO and cMgOP were determined as 10.0 and 10.7, respectively, clearly demonstrating that surface morphologies of cMgOP were changed (see Supplementary Fig. S1). As the sorbents possess positive charge over pH_{zpc}, it thereby can be suggested that removing fluoride by cMgOP is a chemisorption dominated reaction due to electrostatic attraction between the positive surface and negatively charged fluoride ions, similar to a previous report [24].

XRD patterns of MgO (see Supplementary Fig. S2a) and cMgOP (see Supplementary Fig. S2b) show that the two samples form a type of MgO crystal. XRD also indicated that the intensity of characteristic peaks was decreased while the peak area was broadened in cMgOP relative to MgO. The changes in the XRD pattern can be ascribed to the water-dissolved pullulan forming molecular layers around some MgO particles before being calcined while the other maintains pure MgO crystal. When this mixture was calcined, MgO particles would be dispersed by the surrounding pullulan, therefore, the particle size would become smaller leading to a decrease in peak intensity but a larger peak area.

3.2. Effect of contact time on fluoride sorption

The amount of fluoride removed (mg/kg) by cMgOP, MgO and pullulan at an initial fluoride concentration of 10 mg/L is presented in Supplementary Fig. S3. The results revealed that the adsorption of the three adsorbents increased with increasing contact time, and that all three materials were saturated at the 60 min time point. The contact time for subsequent measurements was therefore fixed at 60 min. Our data also indicate that most of the fluorides adsorbed in the first 30 min (over 95%) suggesting less contact time is required for the removal of fluoride from water by cMgOP than for MgO. The defluoridation capacity of cMgOP (4537 mg fluoride/kg) is about 10 times than that of MgO (457 mg fluoride/kg) in the present study, and 1.02 times than MgO/chitosan (4440 mg fluoride/kg) reported previously [18].

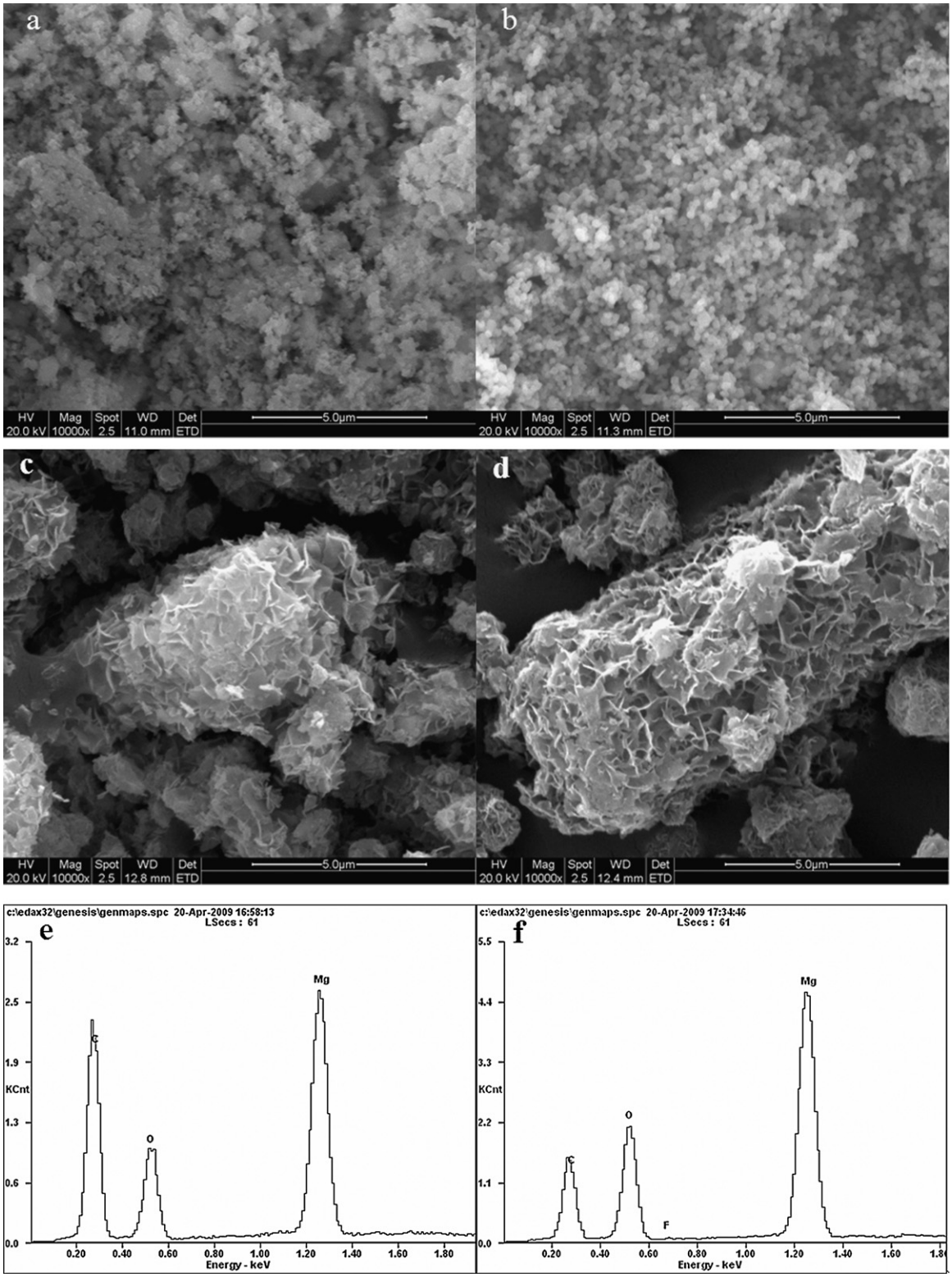

Fig. 2. SEM images of (a) calcining pullulan and (b) calcining MgO, (c) cMgOP, (d) fluoride-sorbed cMgOP, EDAX spectra of (e) cMgOP and (f) fluoride-sorbed cMgOP.

3.3. *Effect of adsorbent dosage on fluoride sorption*

The effect of dosage of cMgOP and MgO on the removal of fluoride at fixed initial fluoride concentration is illustrated in Supplementary Fig. S4. The data clearly showed that the removal efficiency of fluoride was increased with increasing adsorbent dosage in both cases which may be ascribed to the enhanced number of active sites with an increased amount of adsorbent [25]. It can also be seen from supplementary Fig. S4 that there was a sharp increase of the amount of fluoride removal when the dosage of cMgOP and MgO was 0.1 g. Thereafter, no significant increase was observed hence 0.1 g was fixed as the optimum dosage for both MgO and cMgOP in subsequent tests. A similar phenomenon has also been observed previously for other adsorbents [18,24]. This result

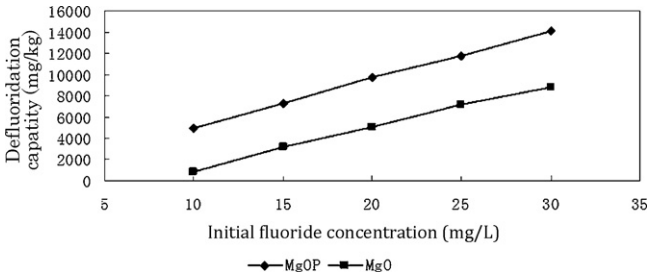

Fig. 3. Effect of different initial fluoride concentrations on defluoridation capacity.

could be interpreted as the better utilization of the available active sites at low adsorbent dose. In contrast, at high adsorbent dose, the relative lower equilibrium concentration of fluoride contributing to the driving force for adsorption may become negligible. The percentage of fluoride removed with a dosage of 0.1 g, was determined to be 90% and 10% for cMgOP and MgO, respectively. Thereby the defluoridation capacity of cMgOP is higher than MgO.

3.4. Influence of pH on fluoride sorption

The uptake of fluoride by cMgOP and MgO was investigated in the pH range from 2 to 12, keeping other parameters constant (see Supplementary Fig. S5). A maximum defluoridation capacity of 97.6% was obtained with a solution of pH 5.0. The percent adsorption was slightly decreased (from 97.6% to 94.5%) on moving towards the pH_{pzc} (10.7) of the adsorbent while at pH above pH_{pzc} the percentage fluoride removal was observed to decrease sharply. The progressive reduction of fluoride uptake could be due to changes in the surface charge of MgOP. If the surface charge of the MgOP was to decrease continuously with the increasing concentration of OH^-, the attractive interactions between the F^- and the adsorbent surface could be adversely affected. When the solution pH is greater than the pH_{zpc}, the total surface charge of the adsorbent becomes negative and hence generating a repulsive interaction between the adsorbent surface and the fluoride ions. Furthermore, the abundance of OH^- ions may also lead to increased hindrance to diffusion of fluoride ions [26]. This could result in the sharp decrease in adsorption capacity at pH higher than pH_{zpc} (see supplementary Fig. S5).

3.5. Effect of initial fluoride concentration on adsorption

The effect of initial concentration on the uptake of fluoride by MgO and cMgOP was studied with initial fluoride concentrations ranging from 10 to 30 mg/L, all other parameters were held constant. The results showed that the defluoridation capacity of both sorbents increased with increasing initial fluoride concentration (Fig. 3). This may be due to the fact that a higher concentration gradient was formed in the presence of more fluoride ions. An increased availability of fluoride ions in solution at the solid–solution interface also enhances adsorption performance [25]. As cMgOP clearly exhibits higher defluoridation capacity than MgO, further investigations were limited to cMgOP only.

3.6. Effect of co-existing ions on fluoride sorption

Some anions that are usually present in fluoride-contaminated drinking water may interfere with the adsorption process. Hence the present study experimentally determined the defluoridation capacity of cMgOP in the presence of common anions such as Cl^-, SO_4^{2-}, NO_3^- and HCO_3^-. In these experiments the initial concentrations of the ions ranged from 100 to 500 mg/L with all other parameters kept constant. Removal efficiencies in the presence Cl^-, SO_4^{2-}, NO_3^-, and HCO_3^- anions are shown in Fig. 4. Cl^-, SO_4^{2-} and NO_3^- were seen to have a positive effect on F^- removal performance while HCO_3^- had a negative effect. It is well-known that Cl^-, SO_4^{2-} and NO_3^- can interfere in Fluorine reagent spectrophotometry, as in present case, they showed a small positive effect. The reduction in fluorine adsorption in the presence of Cl^-, SO_4^{2-} and NO_3^- is, however, sufficiently small as to be negligible. The defluoridation capacity decreases in the presence of HCO_3^-; this may be due to the competition of bicarbonate ions with fluoride ions in the sorption process [13,18].

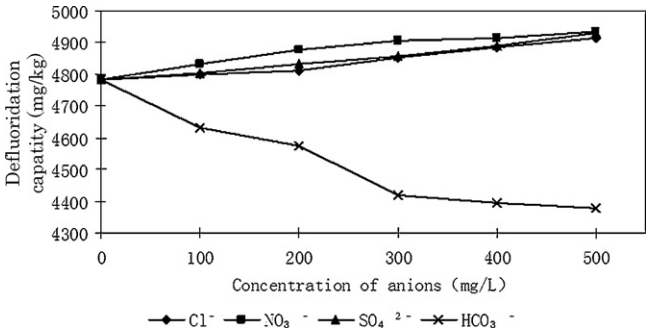

Fig. 4. Effect of some anions on the defluoridation capacity of cMgOP.

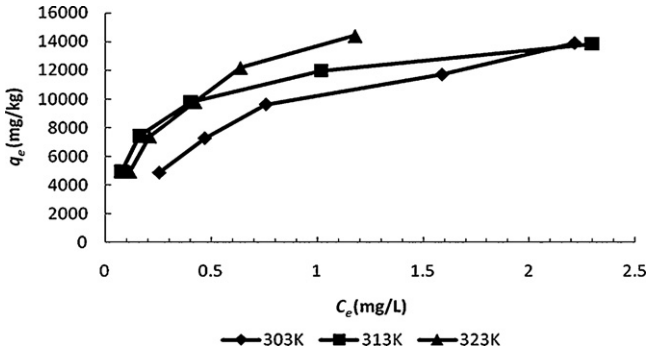

Fig. 5. Adsorption isotherms of fluoride by cMgOP at different temperatures.

3.7. Equilibrium modeling

Adsorption isotherms are basic requirements for the design of sorption systems. These data provide information about the capacity of the adsorbent or the amount required for removing a unit mass of pollutant under the system conditions. The equilibrium adsorption isotherms experiments were performed by plotting fluoride adsorbed (q_e) against the equilibrium concentration of fluoride (C_e) in solution (Fig. 5). Apparently, the adsorption of fluoride was increased as the reaction temperature was raised.

The isotherm models of Freundlich and Langmuir were adopted to fit the experimental adsorption equilibrium data of fluoride on cMgOP. The isotherms profiles of these models are represented in Figs. 6 and 7. From these figures it can be seen that the data comes from experiment fit the Langmuir isotherm model a bit better than Freundlich's isotherm model. The isotherms and the linear forms of these models are represented mathematically as shown in Table 1.

Table 1
Isotherm models and their linear forms.

Isotherms	Linear form	Plot
Freundlich $q_e = k_F C_e^{1/n}$	$\log q_e = \log k_F + \frac{1}{n} \log C_e$	$\log q_e$ vs. $\log C_e$
Langmuir $q_e = Q^0 b C_e / 1 + b C_e$	$C_e/q_e = (1/Q^0 b) + (Ce/Q^0)$	$\frac{C_e}{q_e}$ vs. C_e

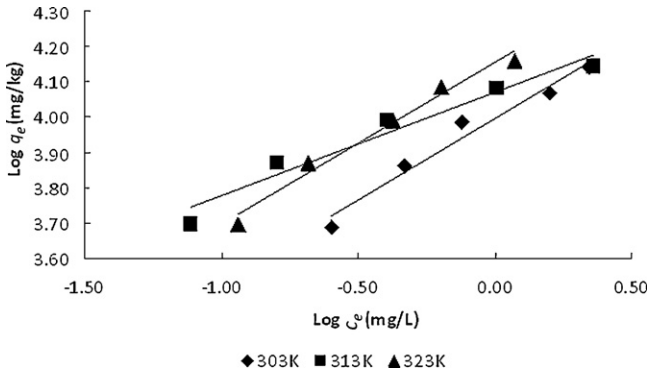

Fig. 6. The Freundlich isotherms profile of the adsorbtion of fluoride by cMgOP.

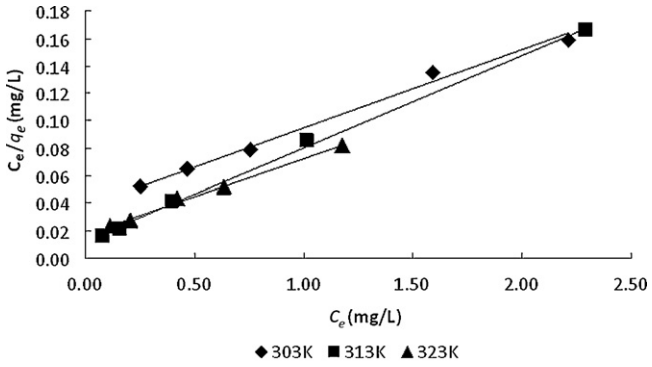

Fig. 7. The Langmuir isotherms profile of the adsorbtion of fluoride by cMgOP.

When the data were analyzed using the Freundlich isotherm [27], the linear plot of log q_e vs. log C_e indicated the applicability of this model. k_F and $1/n$, the constants which relate to the measurement of adsorption capacity and adsorption intensity respectively, are listed in Table 2. The values of $1/n$ ranged from 0 to 1 while the n-values fell within the range of 1–10 (see Table 2), thereby confirming the favorable conditions for adsorption [7]. Additionally, it is evident that fluoride uptake by cMgOP is an endothermic process as an increase in temperature caused an increase in the fluoride adsorption capacity k_F. When the data were analyzed using the Langmuir isotherm [28], the linear plot of C_e/q_e vs. q_e indicated the applicability of Langmuir's isotherm. The constants Q_0 and b are related to sorption capacity and sorption energy, respectively (Table 3). The maximum sorption capacity (Q_0) represents a monolayer coverage of sorbent with sorbate and represents the energy of sorption and should vary with temperature [29].

Table 2
Freundlich isotherm parameters of fluoride sorption on cMgOP with r- and χ^2-values.

Temperature (K)	Freundlich's isotherm				
	$1/n$	n	k_F	r	χ^2
303	0.4623	2.163	9878.7	0.985	171.84
313	0.2924	3.420	11697.7	0.976	261.49
323	0.4577	2.185	14246.2	0.989	143.97

Table 3
Langmuir's isotherm parameters of fluoride sorption on cMgOP with r- and χ^2-values.

Temperature (K)	Langmuir's isotherm			
	Q^0	b	r	χ^2
303	17543.86	1.516	0.998	58.06
313	13698.63	7.300	0.998	84.89
323	17452.00	3.371	0.998	63.10

Table 4
Thermodynamic parameters.

Thermodynamic parameters	Equations	Plot
Standard free energy	$\Delta G^\circ = -RT\ln K_0$	$K_0 = q_e/C_e$
Standard enthalpy change Standard entropy change	$\ln K_0 = \frac{\Delta H^\circ}{RT} + \frac{\Delta S^\circ}{R}$	$\ln K_0$ vs. $1/T$

Note: ΔG° is free energy of sorption (kJ/mol), K_0 is the sorption equilibrium constant, T is the absolute temperature in Kelvin, R is the universal gas constant (8.314 J mol^{-1} K^{-1}), ΔH° is the standard enthalpy change (kJ/mol), and ΔS° is the standard entropy change (J mol^{-1} K^{-1}).

To identify a suitable isotherm model for the sorption of fluoride on cMgOP, the χ^2 test was performed as following:

$$\chi^2 = \sum \left(\frac{(q_e - q_{e,m})^2}{q_{e,m}} \right)$$

where $q_{e,m}$ is the equilibrium capacity calculated according to the model and q_e is the experimental equilibrium capacity. If data from model were similar to the experimental data, χ^2 would be a small number and vice versa. As presented in Tables 2 and 3, the lower χ^2-values obtained when fitting the data using the Langmuir isotherm indicate this model is significantly better than the Freundlich isotherm for describing the fluoride sorption on cMgOP, and also indicating monolayer chemisorption is dominant during the sorption process.

3.8. Thermodynamic investigations

To evaluate the thermodynamic feasibility and further analyze the nature of the adsorption process three basic thermodynamic parameters, standard free energy (ΔG°), standard enthalpy change (ΔH°) and standard entropy change (ΔS°) were calculated [27,30] using the equations listed in Table 4. The values of the thermodynamic parameters are shown in Table 5. The K_0 equals to the fluoride adsorbed per kg sorbent divided by the equilibrium concentration of the solution. It comes from the equilibrium experiment data at initial concentration of the fluoride 25 mg/L at different temperatures. ΔH° and ΔS° can be calculated from the slope and intercept of the plot of $\ln K_0$ versus $1/T$, respectively. The negative value ΔG° confirms the feasibility and the spontaneous nature of the fluoride sorption. The value of ΔH° is 581.33 kJ mol^{-1}, indicating the endothermic nature of the sorption process. The value of ΔS° is determined as 93.158 kJ mol^{-1} K^{-1} indicating the increasing randomness during the sorption of fluoride ions at the solid/liquid.

3.9. Sorption kinetic models

Reaction-based and diffusion-based models [31] were adopted to investigate the sorption dynamics. A relatively higher r-value indicated the better applicability of a pseudo-second-order model (Table 6).

Table 5
Thermodynamic parameters of fluoride sorption on MgOC composite.

Thermodynamic parameters	MgOP composite
ΔG°	
303 K	−22.44 kJ mol^{-1}
313 K	−24.39 kJ mol^{-1}
323 K	−26.48 kJ mol^{-1}
ΔH°	0.58 kJ mol^{-1}
ΔS°	0.093 kJ mol^{-1} K^{-1}

Table 6
Kinetic models and their linear forms.

Kinetic models	Linear form	Plot
Reaction-based		
Pseudo-first-order	$\log(q_e - q_t) = \log q_e - (k_{ad}/2.303)t$	$\log(q_e - q_t)$ vs. t
Pseudo-second-order	$(t/q_t) = (1/h) + (t/q_e)$	t/q_t vs. t
Diffusion-based		
Particle diffusion	$\ln(1 - (C_t/C_e)) = -k_P t$	$\ln(1 - (C_t/C_e))$ vs. t
Intraparticle diffusion	$q_t = k_i t^{1/2}$	q_t vs. $t^{1/2}$

3.9.1. Reaction-based models

Pseudo-first-order and pseudo-second-order models [32] (Table 6) were applied to describe the solid–liquid adsorption process. In Table 6, q_e and q_t are the amounts of fluoride adsorbed on the adsorbent at equilibrium (mg/g) and at time t (min), C_e is the equilibrium concentration (mg/L), C_t is the concentration at time t (mg/L), h is the initial sorption rate (mg/g min), k_{ad} is the rate constant, and k is the pseudo-second-order rate constant (g/mg min). The values of k_{ad} calculated using the pseudo-first-order equation under different experimental conditions are listed in Table 7. There are four types of linear pseudo-second-order kinetic models [33], here we adopted only the most popular linear form (Table 6). Analysis of the model fit showed that our data are better described using a pseudo-second-order model (Table 7).

3.9.2. Diffusion-based models

In a solid–liquid sorption process, the solute transfer is usually characterized either by particle diffusion [34] or intraparticle diffusion control [35]. Equations for the particle diffusion and the intraparticle diffusion models are given in Table 6. k_p is the particle rate constant (min^{-1}). The value of particle rate constant is obtained by calculating the slope of the plot $\ln(1 - C_t/C_e)$ against $t^{0.5}$. If the plot of $\ln(1 - C_t/C_e)$ against $t^{0.5}$ yields a straight-line, it can be concluded that the rate-limiting step is particle diffusion controlled. If the plot of solute sorbed (q_t) against square root of contact time ($t^{0.5}$) yields a straight-line then the rate-limiting step is intraparticle diffusion (or pore diffusion) controlled. As to the intraparticle diffusion model, k_i is the intraparticle rate constant (mg/g $min^{0.5}$). The slope of the plot of q_t against $t^{0.5}$ will give the value of the intraparticle rate constant. The straight-line plots of $\ln(1 - C_t/C_e)$ vs. t and q_t vs. $t^{0.5}$ indicate the applicability of both particle and intraparticle diffusion models. The k_p, k_i and r-values of particle and intraparticle diffusion models are illustrated in Table 7. The higher r-values indicate that the particle diffusion model is best used to describe the adsorption of fluoride on cMgOP.

Table 7
The parameters of various kinetic models with r-values.

Kinetic models	Parameters	10 mg/L	15 mg/L	20 mg/L	25 mg/L
Pseudo-first-order	k_{ad} (min^{-1})	0.0352	0.0332	0.0332	0.0343
		0.0332	0.0339	0.0341	0.0339
		0.0348	0.0343	0.0351	0.341
		0.963	0.963	0.881	0.923
	r	0.854	0.933	0.932	0.904
		0.875	0.913	0.938	0.921
		5.139	7.740	10.341	12.422
	q_e (mg/kg)	5.128	7.776	3.717	12.156
		5.123	7.758	10.163	12.739
		0.0783	0.0338	0.0337	0.0281
	k (g/mg min)	0.0975	0.0471	0.0361	0.0312
		0.1010	0.0528	0.0463	0.0311
Pseudo-second-order	h (mg/kg min)	2.067	2.027	3.609	4.342
		2.563	2.847	3.717	4.888
		2.657	3.181	4.787	5.040
		0.999	0.999	0.999	0.999
	r	0.999	0.999	0.999	0.999
		0.999	0.999	0.999	0.999
	k_p(min^{-1})	0.0125	0.0272	0.0487	0.059
		0.0260	0.0243	0.0187	0.0336
Particle diffusion	r	0.0237	0.0286	0.0439	0.0459
		0.972	0.958	0.978	0.971
		0.953	0.893	0.981	0.969
		0.951	0.949	0.924	0.876
		0.2195	0.4367	05475	0.6352
	k_i (mg/kg $min^{0.5}$)	0.2297	0.3903	0.5054	0.6270
Intraparticle diffusion	r	0.2206	0.3733	0.4245	0.6199
		0.934	0.943	0.882	0.909
		0.768	0.873	0.882	0.861
		0.840	0.871	0.874	0.862

Note: As to the data from each parameter, row 1, row 2 and row 3 were obtained at 303 K, 313 K, and 323 K, respectively.

4. Conclusions

cMgOP, a novel adsorbent, prepared by calcining MgO with pullulan was found to possess excellent defluoridation capacity. The defluoridation capacity of cMgOP was showed only a small variation in the pH range 2–10. The presence of Cl^-, SO_4^{2-} and NO_3^- lead to negligible change in defluoridation capacity, however the presence of HCO_3^- decreased the defluoridation capacity significantly. The sorption of fluoride on cMgOP followed Langmuir isotherm and was spontaneous and endothermic in nature. The rate of sorption closely followed the pseudo-second-order kinetic model and can be characterized by the particle diffusion model. The mechanism of fluoride removal by cMgOP involves both electrostatic attraction and hydrogen bonding. With the high F^- removal efficiency, the ability to be shaped into any desired form and excellent penetrability for water, cMgOP has a good potential to be used as an effective adsorbent in water treatment for defluoridation. However, the treated water was found to be alkaline in nature which may due to the release of Mg^{2+} from cMgOP, thereby a subsequent process would be needed.

Acknowledgements

This work was financially supported by the foundation of Talent Introduction of Huazhong University of Science and Technology (No. 0124261003), the foundation of Youth Science and Technology Chen-guang project of Wuhan (No. 200950431172), the Natural Science Foundation of Hubei Province (No. 2009CDB167), and the National Natural Science Foundation of China (No. 31000030).

Appendix A. Supplementary data

Supplementary data associated with this article can be found, in the online version, at doi:10.1016/j.cej.2010.11.031.

References

[1] T.J. Sorg, Treatment technology to meet the interim primary drinking water regulations for inorganics, J. Am. Water Works Assoc. 702 (1978) 105–111.
[2] M. Srimurali, A. Pragathi, J. Karthikeyan, A study on removal of fluorides from drinking water by adsorption on to low-cost materials, Environ. Pollut. 99 (1998) 285–289.
[3] WHO Guidelines for Drinking Water Quality, vol. 2, 2nd ed., WHO, Geneva, 1996.
[4] M. Yang, Y. Zhang, B. Shao, R. Qi, H. Myoga, Precipitative removal of fluoride from electronics wastewater, J. Environ. Eng. 127 (2001) 902–907.
[5] Y. Ku, H.M. Chiou, W. Wang, The removal of fluoride ion from aqueous solution by a cation synthetic resin, Sep. Sci. Technol. 37 (2002) 89–103.
[6] G.H. Zhang, Y. Gao, Y. Zhang, P. Gu, Removal of fluoride from drinking water by a membrane coagulation reactor (MCR), Desalination 77 (2005) 143–155.
[7] Y. Ku, H.M. Chiou, The adsorption of fluoride ion from aqueous solution by activated alumina, Water Air. Soil Pollut. 133 (2002) 349–360.
[8] Z. Amor, B. Bariou, N. Mameri, M. Taky, S. Nicolas, A. Elmidaoui, Fluoride removal from brackish water by electrodialysis, Desalination 133 (2001) 215–223.

[9] S. Ghorai, K.K. Pant, Investigation on the column performance of fluoride adsorption by activated alumina in a fixed bed, Chem. Eng. J. 98 (2004) 165–173.
[10] K. Muthukumaran, N. Balasubramanian, T.V. Ramakrishna, Removal of fluoride by chemically activated carbon, Ind. J. Environ. Protec. 15 (1995) 514–517.
[11] S.A. Wasay, J.M. Haron, S. Tokunaga, Adsorption of fluoride, phosphate and arsenate ions on lanthanum-impregnated silica gel, Water Environ. Res. 68 (1996) 295–300.
[12] Y. Min, T. Hashimoto, N. Hoshi, H. Myoga, Fluoride removal in a fixed bed packed with granular calcite, Water Res. 33 (1999) 3395–3402.
[13] G. Karthikeyan, A. Pius, G. Alagumuthu, Fluoride adsorption studies of montmorillonite clay, Indian J. Chem. Technol. 12 (2005) 263–272.
[14] Y. Cengeloglu, K. Esengul, M. Ersoz, Removal of fluoride from aqueous solution by using red mud, Sep. Sci. Technol. 28 (2002) 81–86.
[15] A.M. Raichur, M. Jyoti Basu, Adsorption of fluoride onto mixed rare earth oxides, Sep. Purif. Technol. 24 (2001) 121–127.
[16] V.P. Thergaonkar, W.G. Nawalakhe, Activated magnesia for fluoride removal, Ind. J. Environ. Health 16 (1971) 241–243.
[17] D. Zhou, M. He, Y. Zhang, M. Huang, Y. Jiang, Asymmetric hydrogenation of diketones catalyzed by magnesium oxide supported chitosan–Rh complex, Polym. Adv. Technol. 14 (2003) 287–291.
[18] C.S. Sundaram, N. Viswanathan, S. Meenakshi, Defluoridation of water using magnesia/chitosan composite, J. Hazard Mater. 163 (2009) 618–624.
[19] D. Zhou, L. Zhang, S. Guo, Mechanisms of lead biosorption on cellulose/chitin beads, Water Res. 39 (2005) 3755–3762.
[20] Y. Nakano, K. Takeshita, T. Tsutsumi, Adsorption mechanism of hexavalent chromium by redox with condensed-tannin gel, Water Res. 35 (2001) 496–500.
[21] M.V. Lopez-Ramon, F. Stoeckli, C. Moreno-Castilla, F. Carrasco-Marin, On the characterization of acidic and basic surface sites on carbons by various techniques, Carbon 37 (1999) 1215–1221.
[22] T. Noguchi, FTIR detection of water reactions in the oxygen-evolving centre of photosystem II, Philos. Trans. R. Soc. Lond. B. Biol. Sci. 363 (2008) 1189–1194.
[23] Y.S. Al-Degs, M.I. El-Barghouthi, A.A. Issa, M.A. Khraisheh, G.M. Walker, Sorption of Zn(II), Pb(II) and Co(II) using natural sorbents: equilibrium and kinetic studies, Water Res. 40 (2006) 2645–2658.
[24] S.P. Kamble, P. Dixit, S.S. Rayalu, N.K. Labhsetwar, Defluoridation of drinking water using chemically modified bentonite clay, Desalination 249 (2009) 687–693.
[25] A. Mellah, S. Chegrouche, The removal of zinc from aqueous solutions by natural bentonite, Water Res. 31 (1997) 621–629.
[26] A.R. Tembhurkar, S. Dongre, Studies on fluoride removal using adsorption process, J. Environ. Sci. Eng. 48 (2006) 151–156.
[27] H.M.F. Freundlich, Über die adsorption in lösungen, Z. Phys. Chem. 57A (1906) 385–470.
[28] I. Langmuir, The constitution and fundamental properties of solids and liquids, J. Am. Chem. Soc. 38 (1916) 2221–2295.
[29] S. Meeenakshi, N. Viswanathan, Identification of selective ion exchange resin for fluoride sorption, J. Colloid Interface Sci. 308 (2007) 438–450.
[30] A.A. Khan, R.P. Singh, Adsorption thermodynamics of carbofuran on Sn (IV) arsenosilicate in H^+, Na^+ and Ca^{2+} forms, Colloids Surf. 24 (1987) 33–42.
[31] Y.S. Ho, J.C.Y. Ng, G. McKay, Kinetics of pollutant sorption by biosorbents: review, Sep. Purif. Methods 29 (2000) 189–232.
[32] S. Lagergren, Zur theorie der sogenannten adsorption gelöster stoffe, K. Sven. Vetenskapsakad. Handl. 24 (1898) 1–39.
[33] Y.S. Ho, Second order kinetic model for the sorption of cadmium onto tree fern: a comparison of linear and non linear methods, Water Res. 40 (2006) 119–125.
[34] D. Wankasi, M. Horsfall, A.I. Spiff, Retention of Pb(II) ion from aqueous solution by nipah palm (Nypa fruticans wurmb) petiole biomass, J. Chil. Chem. Soc. 50 (2005) 691–696.
[35] W.J. Weber, J.C. Morris, Equilibria and capacities for adsorption on carbon, J. Sanitary Eng. Div. 90 (1964) 79–91.